



UNIVERSITY OF LEEDS

This is a repository copy of *Influence of matric suction on resilient modulus and CBR of compacted Ballina clay*.

White Rose Research Online URL for this paper:

<https://eprints.whiterose.ac.uk/192884/>

Version: Accepted Version

Article:

Lim, S-M, Indraratna, B, Heitor, A orcid.org/0000-0002-2346-8250 et al. (4 more authors) (2022) Influence of matric suction on resilient modulus and CBR of compacted Ballina clay. *Construction and Building Materials*, 359. 129482. ISSN 0950-0618

<https://doi.org/10.1016/j.conbuildmat.2022.129482>

© 2022 Elsevier Ltd. All rights reserved. © 2022, Elsevier. This manuscript version is made available under the CC-BY-NC-ND 4.0 license <http://creativecommons.org/licenses/by-nc-nd/4.0/>.

Reuse

This article is distributed under the terms of the Creative Commons Attribution-NonCommercial-NoDerivs (CC BY-NC-ND) licence. This licence only allows you to download this work and share it with others as long as you credit the authors, but you can't change the article in any way or use it commercially. More information and the full terms of the licence here: <https://creativecommons.org/licenses/>

Takedown

If you consider content in White Rose Research Online to be in breach of UK law, please notify us by emailing eprints@whiterose.ac.uk including the URL of the record and the reason for the withdrawal request.



eprints@whiterose.ac.uk
<https://eprints.whiterose.ac.uk/>

1 **Influence of Matric Suction on Resilient Modulus and CBR of Compacted**

2 **Ballina Clay**

3 Sin-Mei Lim^b, Buddhima Indraratna^c, Ana Heitor^d, Kai Yao^{a*}, Dalong Jin^e, Wael M.

4 Albadri^f, Xia Liu^g

5 ^a School of Qilu Transportation, Shandong University, Jinan 250002, China.

6 ^b NUS Environmental Research Institute (NERI), National University of Singapore, 21 Lower Kent Ridge Road,
7 Singapore 119077, Singapore.

8 ^c Faculty of Engineering & Information Technology, University of Technology Sydney, Broadway, NSW 2007,
9 Australia.

10 ^d School of Civil Engineering, University of Leeds, LS2 9JT, UK. ^e Department of Civil Engineering, Beijing
11 Jiaotong University, Beijing 100044, China.

12 ^f Department of Mechanical Power Technical Engineering, Al—Amara University College, Misan 62001.

13 ^g Jining Hongxiang Highway Survey Design & Research Institute Co. Ltd, Jining 272000, China.

14
15 ***Corresponding author (Kai Yao)**

16 Email addresses: drsinmei@gmail.com (Sin-Mei Lim), Buddhima.Indraratna@uts.edu.au (Buddhima Indraratna),
17 A.Heitor@leeds.ac.uk (Ana Heitor), yaokai@sdu.edu.cn (Kai Yao), jindalong@163.com (Dalong Jin),
18 w_m120@yahoo.com (Wael M. Albadri), 838052903@qq.com (Xia Liu)

19
20 **Abstract:** Road infrastructure is often built above the groundwater table. The materials
21 used are usually compacted and thus generally remain under unsaturated conditions
22 throughout their service life. This paper presents experimental results that highlight the
23 influence of matric suction on the resilient modulus (MR) and California bearing ratio
24 (CBR) of a compacted subgrade Ballina clay (typically found in NSW, Australia). The
25 soil specimens were prepared in a range of water contents and dry unit weights, tested
26 using a series of repeated load triaxial tests and CBR tests, and the associated matric
27 suction was measured using the filter paper method. The tests were complemented by
28 the study of the macrostructure of the compacted specimens using X-ray computed
29 tomography (CT). Test results show that there are intimate relationships between the
30 soil suctions and resilient modulus as well as CBR on the compacted clay at different
31 moisture contents and that both parameters can be defined empirically through matric

32 suction. A linear trend was established between matric suction and M_R with a high
33 coefficient of correlation of 0.99. CT scan results reveal that increasing soil moisture
34 increased the inter-pores volume and the aggregations became more compressible and
35 present probable matrix-dominated macrostructure during compaction. While soils
36 compacted at the dry side of optimum moisture content yield distinct aggregations
37 owing to the flocculation and aggregation of soil structure.

38 **Keywords:** Compaction; Matric suction, CT-Scan; CBR, Resilient modulus

39 **Introduction**

40 The mechanical behaviour of an unsaturated pavement subgrade is significantly
41 influenced by the variation of the soil suction [1], with is also known as negative soil
42 pressure due to the cooccurrence of air and water in the soil fabric [2]. It implicitly
43 measures the effect of soil-water interaction forces on the deformation characteristics
44 of the pavement materials [3]. For an unsaturated soil, the association of the soil suction
45 with the surface tension between water and the soil particles is a state variable essential
46 for assessing the mechanical response to loading, in particular under repeated traffic
47 loading [4]. Thus, one of the key mechanical properties for determining the response
48 of pavements under repeated traffic loading according to the Mechanistic-Empirical
49 Pavements Design Guide [5] is the resilient modulus (M_R), along with its susceptibility
50 to changes in water which is corresponding to changes in matric suction. Another most
51 widely used parameters in the design of pavement subgrade is the California bearing
52 ratio (CBR), where the bearing ratio and deformation of the subgrade layers are greatly
53 affected by the changes of matric suction of the soil [6]. Over and above this, field dry
54 unit weight is also another mechanical parameter essential in quantifying the
55 compaction quality of the pavement subgrade, while the associated water content
56 affects the magnitude of matric suction, this successively influence the effective stress
57 of the compacted soil [4]. However, there have been limited studies on the influence
58 of soil suction on CBR in relation to its M_R under the whole range of water content
59 across the compaction curve.

60 Mirzaii and Negahban (2016) [6] discussed extensively on the effects of soil
61 suction with CBR on clayey sand. Recent studies [7, 8] attempts on investigating the
62 effect of matric suction (ψ_m) on resilient modulus (M_R) and found that an increase in
63 ψ_m contributes to the enhancement of soil stiffness for a compacted soil. On the other

64 hand, Kim and Kim (2007) [9] evaluated the resilient modulus of the compacted sandy-
65 silty Indiana subgrade soils prepared at different water contents. Similar nature of
66 research was done by Nowamooz et al. (2011) [10] in investigating the resilient
67 behaviour of a natural compacted sand prepared at various moisture contents, without
68 correlating with soil suction or CBR value. Furthermore, Sawangsurriya et al. (2008)
69 [11] studied the effect of matric suction on M_R of fine-grained subgrade soils
70 compacted at optimum moisture contents (OMC) and note that the M_R increases with
71 the increase in soil matric suction. Several studies were attempted in correlating M_R
72 with CBR on various unsaturated soil type [12-13]. Among others, Garg et al. (2009)
73 [14] opined that a relationship between M_R and CBR can be established but there is a
74 wide divergence from the experimental value. Whereas Leung et al. (2013) [15] re-
75 examined the prediction of M_R with CBR for compacted saprolitic subgrade soils using
76 several models established by past researchers but the result shows that the predicted
77 relationships were either limited to different ranges of compaction density or were
78 excessively conservative for adoption. Leung et al also further emphasize the
79 importance of saturation and moisture ratio, inextricably correspond this to the soil
80 suction that are useful in estimating M_R and CBR. Notwithstanding this, most of the
81 aforementioned studies focuses solely on the correlation of either the soil suction with
82 CBR or M_R , or the relationship of CBR and resilient modulus, these studies did not
83 consider the influence of soil suction on both CBR and M_R arising from the variation
84 in water contents and density in the compacted soil, and its interrelationship.

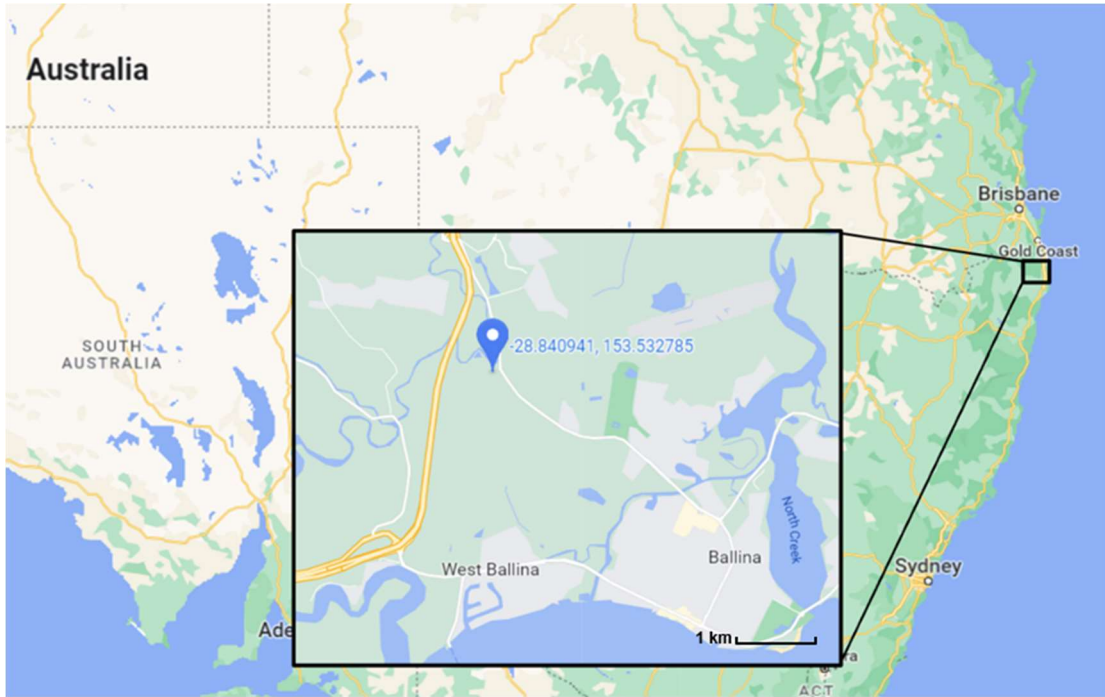
85 This study investigates the influence of soil suctions on the resilient modulus
86 and CBR properties of Ballina clay in its compacted state and their interrelationships
87 through a series of laboratory testing. The study reveals that there is an intimate
88 relationship between the soil suction and resilient modulus as well as CBR arising from

89 its compaction characteristics (i.e. moisture content and dry unit weight). A one-to-one
90 relationship was also observed with the M_R and CBR across the evolution plane based
91 on matric suction. The tests were complemented by the study of the macrostructure of
92 the compacted specimens using X-ray computed tomography (CT).

93

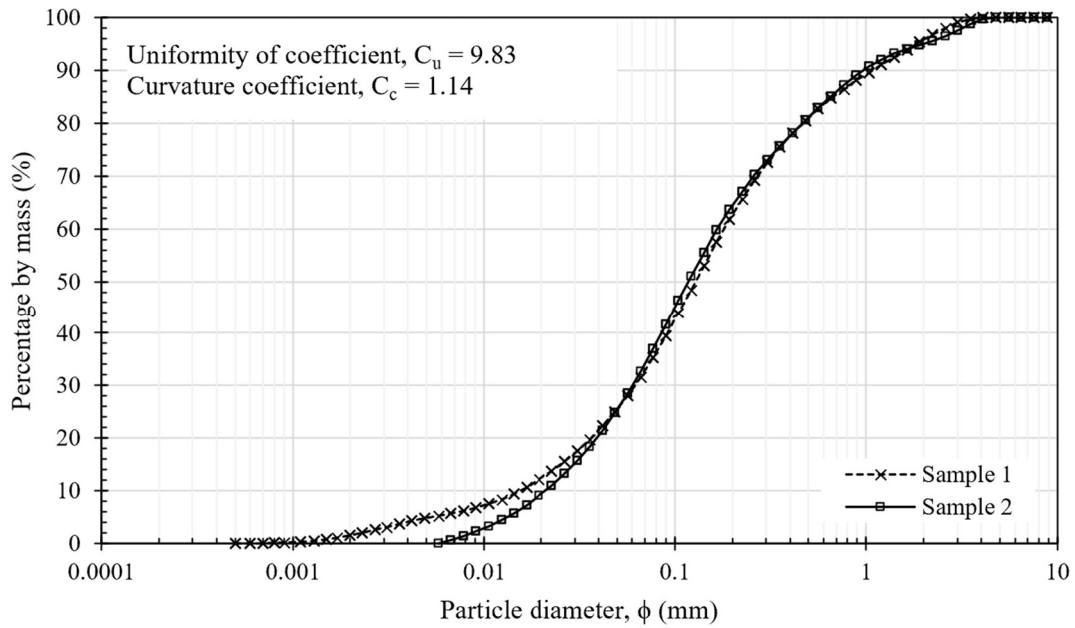
94 **Materials and Testing Strategy**

95 The soil selected for this study was collected from a site close to the Pacific
96 Highway in Ballina which runs along the east coast of Australia between Sydney and
97 Brisbane (Fig. 1). This site, located in a low-lying flood plain, consists of mostly highly
98 compressible and saturated clays. Ballina clay has a liquid limit (LL) of 96%, a
99 plasticity index (PI) of 63% and a specific gravity of 2.63. The particle size distribution
100 of the Ballina clay (Fig. 2) represents approximately 67% sand, 17.25% silt and 11%
101 clay size fraction whereas the uniformity of coefficient (C_u) is 9.83 and curvature
102 coefficient (C_c) is 1.14. Thus, based on the index properties and the grain-size
103 distribution, the soil is classified as high-plasticity clay, CH [16]. Ballina clay can also
104 be classified as CE according to British Soil Classification System (BSCS) where C is
105 defined as clay and E is defined as extremely high ($LL > 90\%$). The soil properties of
106 Ballina clay have also been studied in detail by Indraratna et al. (2014) and Pineda et
107 al. (2016)[17-18] and the basic soil properties are given in Table 1.



108
109
110
111

Fig. 1. Location of Ballina, New South Wales, Australia (inset: Ballina soil sampling location at 28°50'24.2"S and 153°31'58.3"E) [19]



112
113
114

Fig. 2. Particle size distribution of Ballina Clay.

115 **Table 1**
116 Soil properties of Ballina Clay.

Parameters	Unit	Values
Liquid limit, LL	%	94.7
Plastic limit, PL	%	32.2
Plasticity Index, PI	%	62.5
Water content, w	%	92.6
Specific gravity	-	2.63
Void ratio	-	2.36
Wet unit weight, γ_w	kN/m ³	16.5

117

118 Before compaction, the soil sample was air dried prior to mixing with the required
119 amount of water using ORIMAS Universal mixing machine that had a 20L capacity,
120 240V, and at speed of 91 rpm for 2 minutes. Any visible moisture lumps were then
121 disaggregated before placing the moist mixture in a plastic bag kept for moisture
122 equilibration (e.g. under constant temperature and humidity conditions).

123 The compaction characteristics were determined using a Standard Proctor
124 compaction test in accordance to [20]. To determine the maximum dry unit weight and
125 optimum moisture content of Ballina clay, a total of 9 compacted specimens were
126 prepared so that a range of different dry densities could be attained in terms of water
127 content. All the specimens were compacted on the same day to prevent curing
128 differences due to air temperature and humidity fluctuations, which at times can be
129 significant. Compaction energy of $E = 595 \text{ kJ/m}^3$ was adopted for all tests with water
130 content in the selected specimens varied across the compaction plane (12.1% to 25.2%).
131 These specimens were then utilized to mould the material for the CBR test and for the
132 resilient modulus tests using a cyclic triaxial apparatus (e.g. 50mm diameter by 100
133 mm high specimens, following the procedure described by Chen et al., 2015[21].
134 Additional specimens were prepared for determination of soil suction and used for CT-
135 scanning. Soil suction was measured using the filter paper method which is a method

136 that is valuable in deriving both total and matric suction [22]. It should be noted that at
137 least 3 replicate samples were prepared for every test conducted in this study.

138

139 **Resilient modulus and California bearing ratio**

140 The resilient modulus (M_R) values are obtained to measure the degree to which a
141 soil can recover from stress levels commonly placed upon soils by traffic [23]. The aim
142 is to provide a relationship between stress and deformation of a soil material that can
143 be used for the structural analysis of layered pavement systems. The test was conducted
144 at constant water content to simulate typical field conditions. In this study, the resilient
145 modulus is defined as:

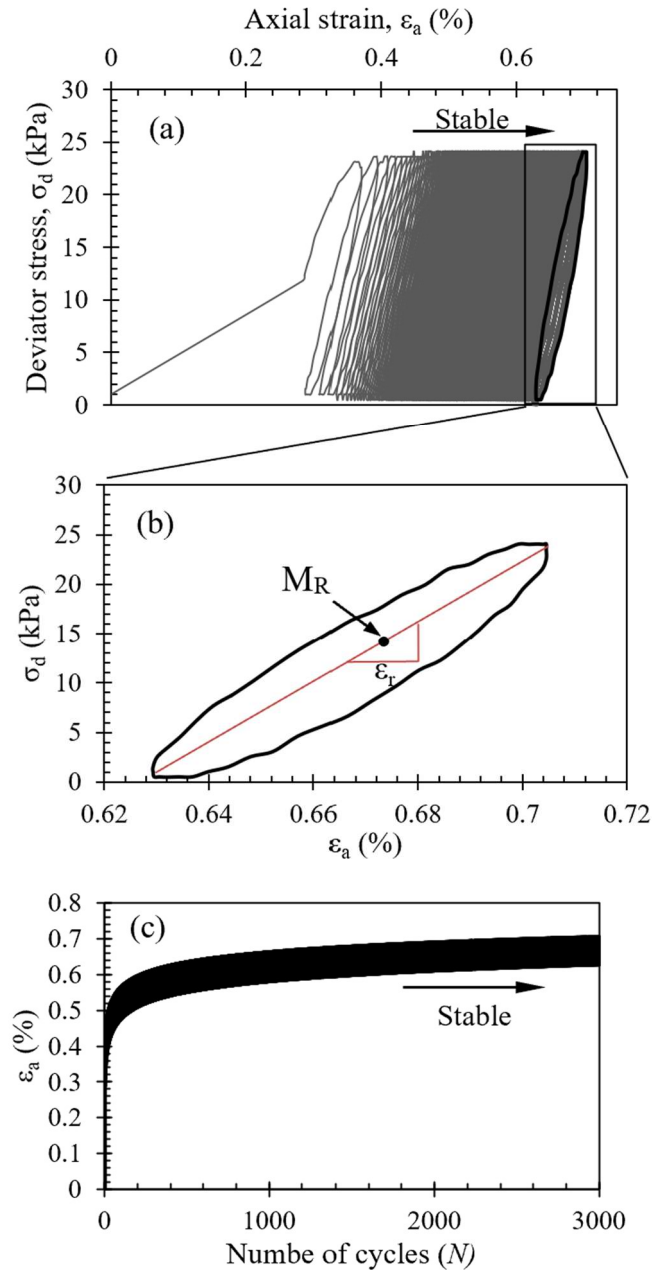
$$146 \quad M_R = \frac{\sigma_d}{\varepsilon_r} \quad (1)$$

147 where M_R is the resilient modulus, σ_d is the cyclic deviator stress, ε_r is the recoverable
148 axial strain. As indicated in Eq. (1), the larger the recoverable deformation, the smaller
149 the resilient modulus. A constant all-around confining pressure (20kPa) is applied on
150 the specimen to simulate the lateral stress caused by the overburden stress and applied
151 wheel load. The suggested level of confining stress on top of the subgrades was in the
152 range of 13.8 kPa to 27.6 kPa which is appropriate for determining M_R for the design
153 of pavement [9]. The confining pressure was controlled using a GDS instruments water
154 pressure controlled (accuracy 1 mm³ and 1 kPa) Resilient modulus tests were carried
155 out by applying a cyclic load having haversine-shaped pulse with duration of 0.1
156 second and rest period of 0.9 seconds. For ensuring the accuracy of the cyclic test
157 results (i.e. axial stress and strain), the data was sampled at a relatively high rate and
158 20 data points were recorded for each cycle.

159 Compacted specimens were loaded according to ASTM D5311[24] method. Fig.
160 3(a) shows a typical deformation response of Ballina clay under repeated loading. At

161 the initial stage of the test, at a relatively small number of cycles ($n < 100$, [Fig. 3c](#)), there
162 is a considerable permanent deformation occurring indicated by the plastic strain.
163 The M_R is calculated as the mean of the last five cycles considering the recoverable
164 axial strain and cyclic deviator stress as shown in [Fig. 3\(b\)](#). The loading involves
165 conditioning, which attempts to establish steady-state or resilient behaviour labelled as
166 'stable' shown in [Fig. 3\(c\)](#), through the application of a large number of cycles (i.e.,
167 3000 cycles). In the similar figure, it can be seen that the recoverable strains occur after
168 numerous load repetitions, it is important to note that the deviator stress applied should
169 not exceed the shear strength of the soils. The bearing capacity of compacted Ballina
170 clay was determined with CBR test. The soil samples were compacted using proctor
171 compaction method (1L mould) and the test procedures followed were in accordance
172 with [ASTM D1883-05 standard \[25\]](#).

173



174

175 **Fig. 3.** A typical resilient modulus measurement technique. Cyclic loading results
 176 showing soil specimen with $\gamma_d=15.9 \text{ kg/m}^3$ and $w=15.5\%$.

177

178 Water retention behaviour

179 The suction-moisture content relationship was obtained using the filter paper
 180 technique in accordance with [ASTM standard D5298 \[26\]](#). The 55 mm Whatman No.
 181 42 ashless filter paper was used in this technique. Two methods were adopted for
 182 measuring suction, i.e. non-contact and contact method for determining total and matric

183 suction, respectively. In the non-contact method, the filter paper is placed either on a
 184 disc above the soil in an airtight container for at least seven days whereas in the contact
 185 method, the filter paper disks are placed in direct contact with the soil. A minimum of
 186 two filter papers determinations were carried out for determining the soil suction for
 187 each compacted specimen prepared at a given water content and dry unit weight (see
 188 Fig. 4) and the average suction value was considered. In this technique, the soil suction
 189 is determined based on the filter paper water content on the basis that a filter paper will
 190 come to equilibrium with respect to moisture flow with the soil after 7 days [27].
 191 ASTM D5298[26] only provides one calibration curve for both matric and total suction
 192 determinations, however there have been many studies that showed that for Whatman
 193 42 filter paper, two sets of calibration should be adopted for matric and total suction
 194 respectively [28].

195 Thus, in this study, soil suction calibration equations follow those proposed by
 196 [34]:

$$197 \quad \text{Log } \psi = a - b w_f \quad (2)$$

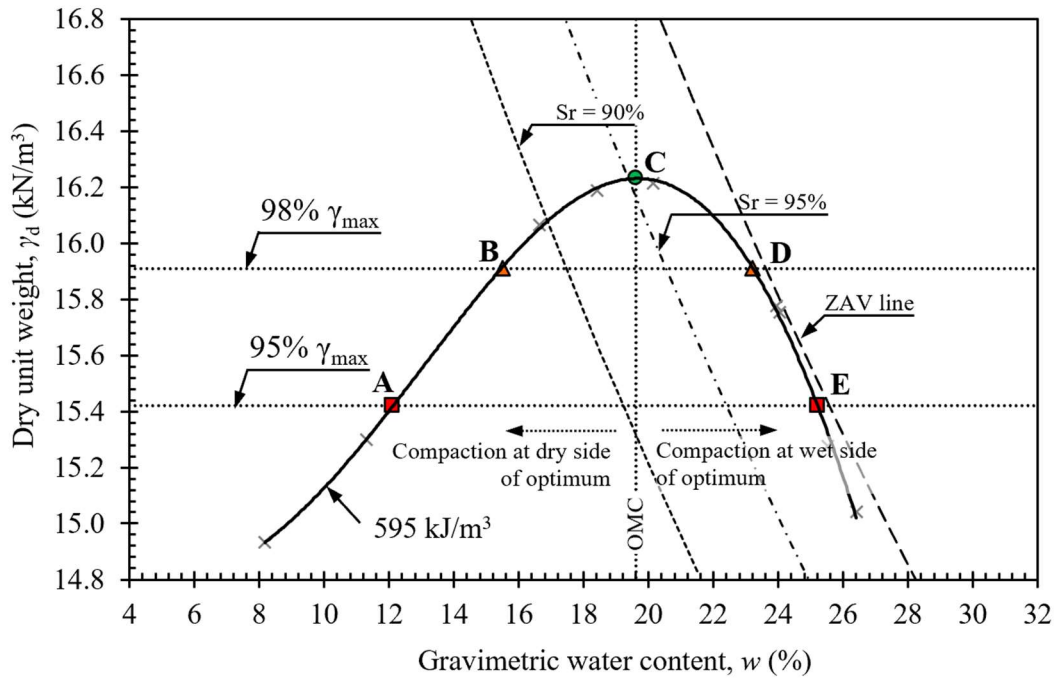
198 Where $\log \psi$ is the logarithm of suction (kPa) in base 10, a and b are constants and w_f
 199 is the filter paper water content at present.

200 The equation was further used and modified through extensive research work
 201 carried out by Leong et al. (2002)[28]. The experimental evidence reported by Leong
 202 et al. (2002)[28] indicates that separate equations, i.e., Eq. (3) to (6) should be used to
 203 determine the matric and total suction.

$$\text{Total suction} \quad \left\{ \begin{array}{ll} w_f < 26; & \log \psi = 5.31 - 0.0879 w_f \quad (3) \\ w_f \geq 26; & \log \psi = 8.778 - 0.222 w_f \quad (4) \end{array} \right.$$

$$\text{Matric suction} \quad \left\{ \begin{array}{ll} w_f < 47; & \log \psi = 4.945 - 0.0673 w_f \quad (5) \\ w_f \geq 47; & \log \psi = 2.909 - 0.0229 w_f \quad (6) \end{array} \right.$$

204 Where w_f is the water content of filter paper and ψ is soil suction. Eq. (3) to (6) was
 205 used in this study to determine the total and matric suction.
 206



207
 208 **Fig. 4.** Compaction curves of Ballina Clay at compaction energy of $E = 595 \text{ kJ/m}^3$.

209

210 Medical grade computed tomography-scanner testing

211 Computed tomography (CT) scanning systems use X-rays to visualize thin, cross
 212 sections of specimens. During CT scanning, high voltage X-rays generated from a
 213 source located at one side of the gantry, are attenuated through the test specimen and
 214 then registered by a series of detectors placed in the opposite direction. As the X-rays
 215 penetrate through the test specimen, some of them are absorbed. The different rates of
 216 absorption reflect changes in the specimen density [29]. The tests were carried out
 217 using an X-ray CT scanner (Toshiba Asteion S4). The reconstruction function adopted
 218 in this study enabled the correction of image artefacts that could result from the absence
 219 of lower energy X-rays. The X-ray tube current and voltage was 200 mA and 135 kV,

220 respectively. The X-ray beam was as per soil slice thickness which is 2 mm wide, the
221 exposure time was allowed at 1 second, and the field of view (FOV) was 75 cm that
222 enable a zooming factor of four. The compacted soil specimens were scanned
223 horizontally at 2-mm interval and the resulting CT scans were then used to create
224 images along vertical planes at a range of 16mm through the center of the soil cylinder.
225 The CT-scan images were analyzed using medical radiology software DicomWorks v.
226 1.3.5. The images not only portray well with the general arrangement of the soil
227 structure but this technique also allows for the specimens to be tested non-intrusively
228 and in “as-compacted” state, without damaging the soil structure.

229

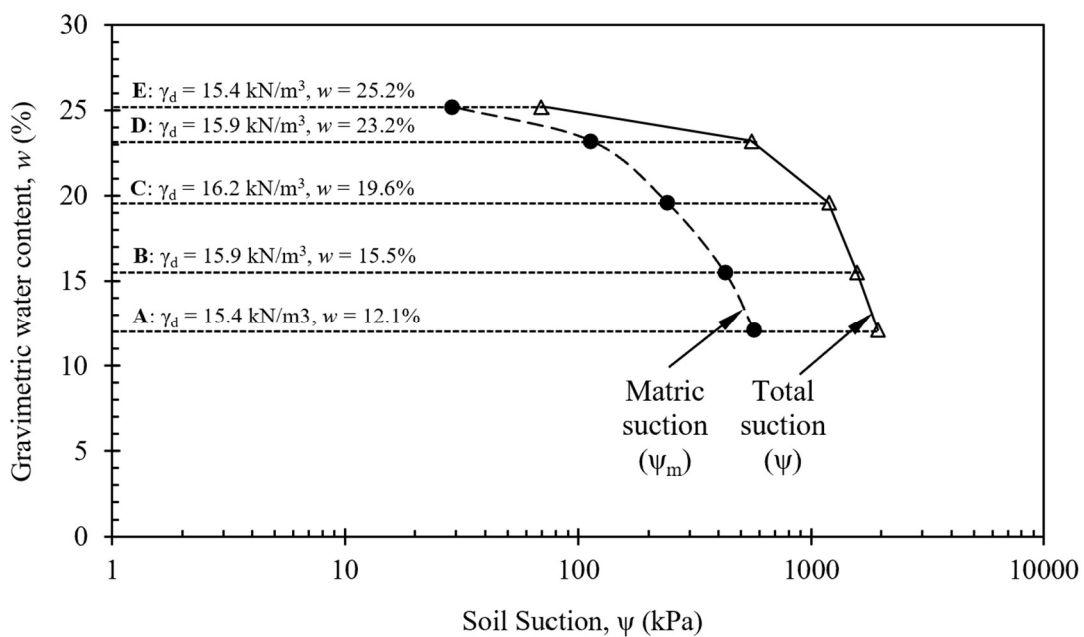
230 **Results and Discussion**

231 **Soil suction and degree of saturation for compacted specimens**

232 [Fig. 4](#) shows the compaction curve for compacted Ballina clay at compaction
233 energy of 595 kJ/m³. The gravimetric water content varied from 12% to 25% at 95%
234 dry unit weight. The maximum dry unit weight and optimum moisture content is 16.2
235 kN/m³ and 19.6%, respectively. For the compaction energy level adopted, the dry unit
236 weight increases as the moisture content increase to the OMC. Beyond this point (i.e.
237 compaction at the wet side of optimum), the dry unit weight decreases with increasing
238 water content. The water retention curves were plotted in [Fig. 5](#) for sample compacted
239 across different water content. As expected, an increase in soil moisture content leads
240 to a decrease in both total and matric suction. As the Ballina clay soil is of marine
241 origin, the difference between matric and total suction is worthy of note in [Fig. 6](#). The
242 presence of some degree of salinity in Ballina Clay is responsible for the difference
243 between total and matric suction as also known as osmotic suction (ψ_π). Interestingly,
244 a hysteretic behaviour is observed where the ψ_π value decreased as the S_r increased

245 indicating that as the soil is closer to saturation and the salt concentration in the soil is
 246 likely reduced and hence a lower osmotic suction is obtained. For higher degree of
 247 saturations, which is shown beyond the dashed line S_e , when most of the soil pores are
 248 filled with water, the effect of salt concentration is likely to be less, and therefore both
 249 matric and total suction are of similar magnitude. In contrast, for specimens that were
 250 prepared at drier water contents this difference becomes larger. The matric suction of
 251 all the 5 specimens ranged from 29 kPa to 567 kPa. [Vullient et al. \(2002\)\[30\]](#) stressed
 252 that the mechanical stress level is affected by the soil suction and greatly influences the
 253 hydric behaviour.

254



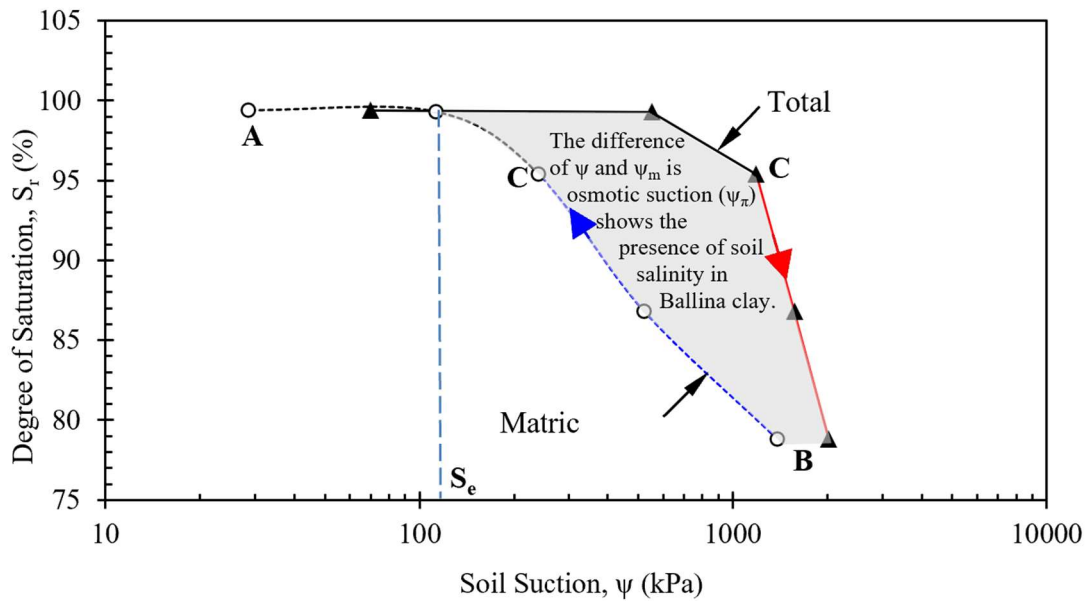
255

256 **Fig. 5.** Water retention curves of compacted Ballina clay at specific dry density and

257

water content measured using filter paper method.

258



259

260

Fig. 6. Variation of soil suction with degree of saturation.

261

262 **The Influence of Matric Suction on California Bearing Ratio (CBR)**

263

264

265

266

267

268

269

270

271

272

273

274

275

The CBR test was carried out to examine the effect of soil moisture content on the bearing capacity of compacted Ballina clay. It can be seen from Fig. 7 that the curves for samples compacted at the dry side of optimum moisture content (OMC), i.e. A and B tend to concave up at the beginning for penetrations typically smaller than 1.5mm. This is likely due to surface irregularities and therefore zero point was adjusted to obtain the accurate CBR value. A bilinear trend was also observed from the load-penetration curves for sample A and B. At relative dry conditions which is below OMC, there was a marked increase in CBR values due to the increase of dry soil unit weights and the CBR reaches a value of 28 and 22.9%, respectively for sample A and B. For a 3.1% decrement of water content for sample B from sample A, the CBR value has a percentage increment of approximately 18%. When the water content increases from 15.5% for sample B to optimum moisture content (19.6%) at pronounced critical points for soil compacted at maximum dry unit weight, the value of CBR decreases to 9.9.

276 The gradient of the load on piston decreases when moisture content of the soil increases.
277 However, the effects became much lesser for specimens prepared on the wet side of
278 the OMC. For specimen D and E, when the moisture content is higher than that of the
279 OMC, the gradient of the load on piston decreases quite steadily to almost constant. On
280 the dry side of OMC, the CBR reaches a value of 28 and 22.9%, respectively for sample
281 A and B. For a 3.1% decrement of water content for sample B, the CBR value has a
282 percentage increment of approximately 18%. Soil compacted at moisture content above
283 OMC could rarely reach a CBR of 5% or above, therefore soil compacted at its OMC
284 was often regarded as competent materials by many design standards [15]. Sample type
285 A and E compacted at the same dry unit weight ($\gamma_d = 15.4 \text{ kN/m}^3$) but at different
286 moisture content i.e. 12.1% and 25.2%, respectively shows an exceptionally large
287 difference in its CBR value, 3.4 compared to 22.9. This indicates that soil water content
288 and associated soil structure on the dry and wet sides of OMC (e.g., [31]) plays the
289 predominant role in the soil strength response evaluated through CBR. Similar
290 observations can be made for specimen B and D. The aforementioned trends observed
291 in this study were corresponding to the findings ascertained by Cabalar & Mustafa
292 (2017)[32].

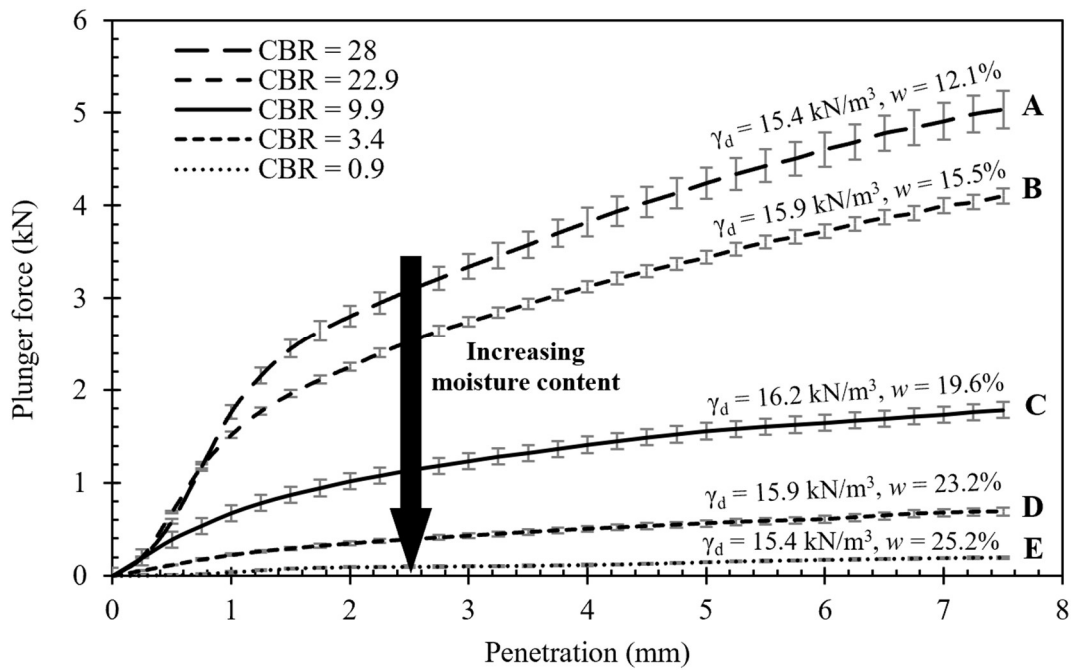


Fig. 7. California Bearing Ratio (CBR) test result curves.

293

294

295

296

297

298

299

300

301

302

303

304

305

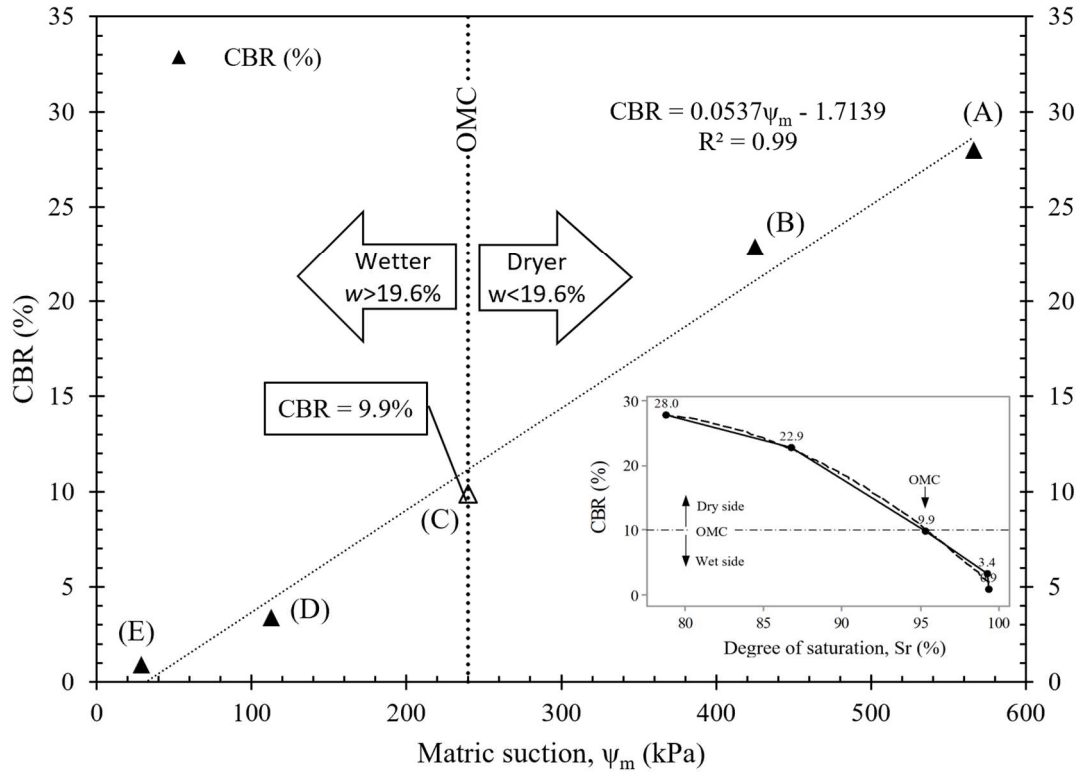
306

307

308

309

While CBR decreased with increasing water content, an opposite trend was observed for matric suction (Fig. 8). This is not surprising as previous studies indicated that suction governs the strength behaviour of compacted soils [3, 33]. Further, there seems to be a linear trend established between the matric suction and CBR, showing a high coefficient of correlation of 0.99. This can be used to readily estimate CBR along the compaction plane provided that matric for the compacted materials is measured. Notwithstanding this, it is worthy of noting the nonlinear relationship observed from the inset of the figure for CBR plotted against the degree of saturation. On the dry side of OMC, the CBR remains approximately around the same order whereas sharply decreases once OMC is exceeded. This behaviour is likely due to the concurrent suction decrease and dry unit weight increase from point A to B (see Fig. 4) and concurrent decrease of suction and dry unit weight that occurs once OMC is exceeded. These observations are in agreement with findings reported by Heitor et al. (2013)[34] for the small-strain shear modulus.



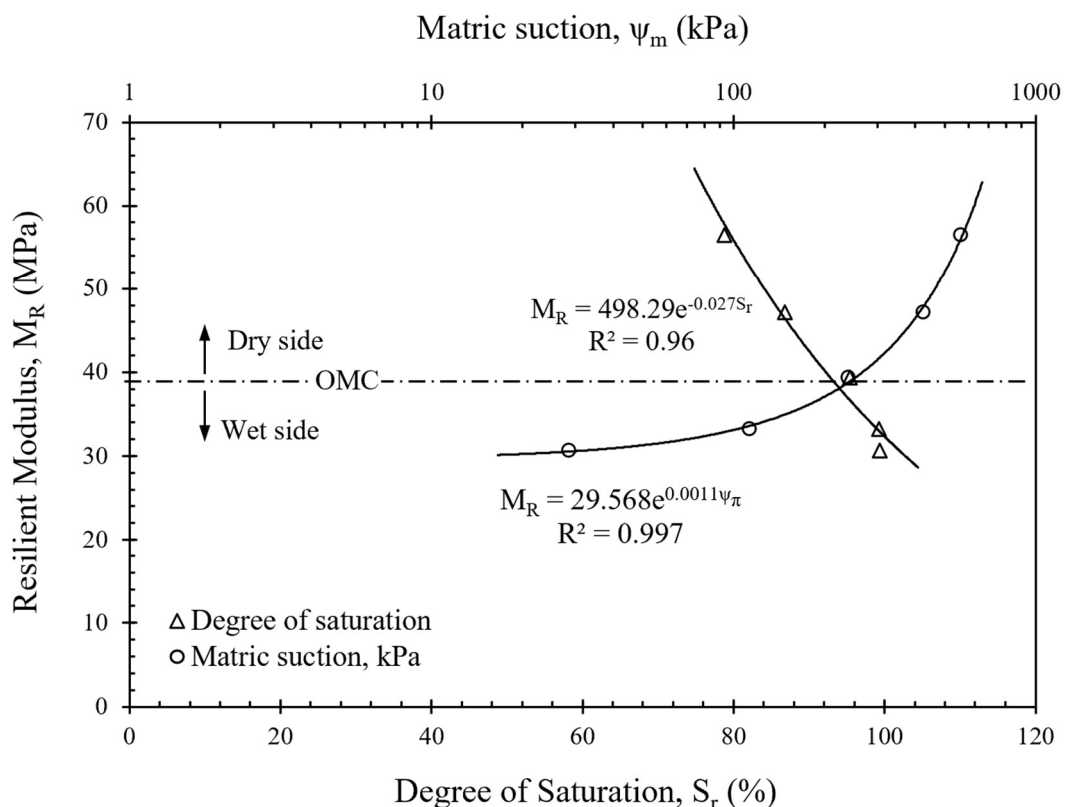
310

311 **Fig. 8.** Evolution of the CBR values based on matric suction at five different water
 312 contents: (A) $w = 12.1\%$, (B) $w = 15.5\%$, (C) $w = 19.6\%$, (D) $w = 23.2\%$ and (E) $w =$
 313 25.2% .

314 **The Influence of Matric Suction on Resilient Modulus**

315 [Fig. 9](#) shows the variation of M_R as a function of S_r and ψ_m , respectively. It was
 316 observed that the M_R of the compacted materials have significant relation to the soil
 317 suction in terms of soil moisture content. Two empirical relationships are proposed for
 318 the prediction of M_R through S_r and ψ_m with high coefficient of determination of 0.95
 319 and 0.90, respectively. The matric suction possesses a better relationship with M_R
 320 compared to soil degree of saturation. This phenomenon is in agreement with findings
 321 reported by Sawangsuriya et al. (2008) [11] and Dong et al. (2020)[8]. Although the
 322 dry unit weight of the specimen compacted as dry side of OMC (15.4kN/m^3) is smaller
 323 than that of specimen compacted at OMC (16.2kN/m^3), the value of M_R is higher which
 324 is 56.5MPa compared to M_R value of 39.3MPa at OMC. This appears to be caused by

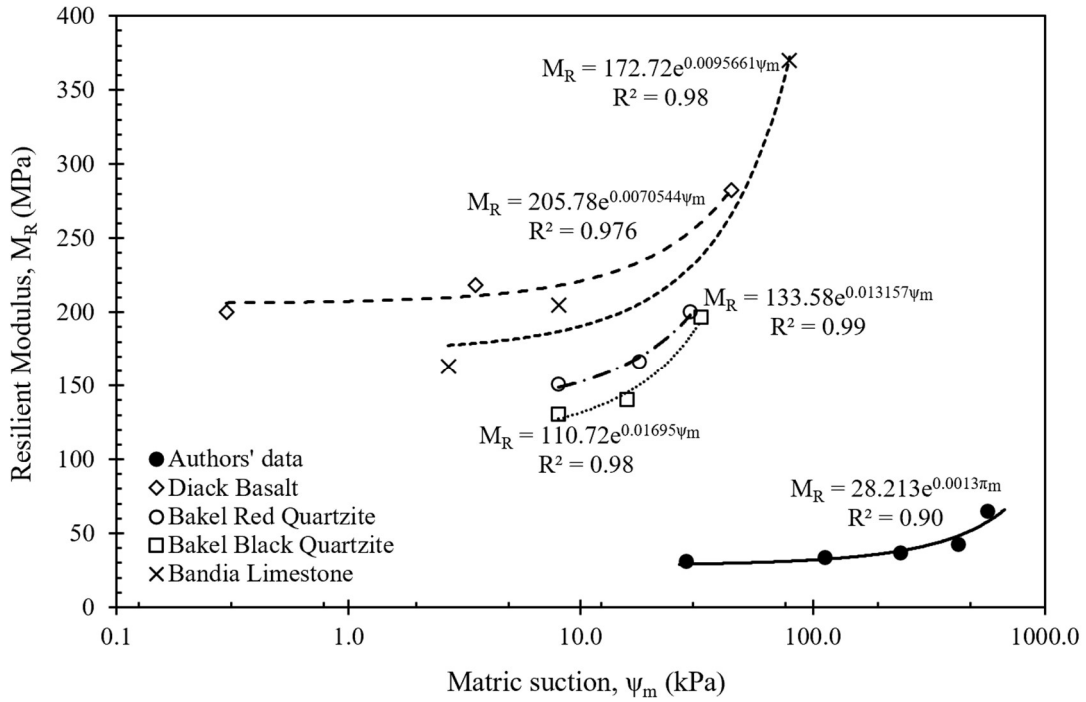
325 capillary suction which contributes to an increase in the effective stress by attracting
 326 particles towards one another and thus exhibiting higher particle contact force that
 327 results in higher M_R values [9]. Moreover, the gradual increase in matric suction
 328 indicates the increase in capillary menisci between the solid particles, resulting in an
 329 increase in inter-capillary forces [2] and, therefore the M_R . Fig. 10 (a) and (b)
 330 illustrates the past literature [2] on resilient modulus with matric suction and degree of
 331 saturation, respectively. Despite of lower M_R values obtained for the Ballina clay used
 332 in this study, it shows the same trend with other types of material used. It also seems
 333 that there is a much less variation at the wet side that coming to a plateau. Similar trend
 334 has been observed by [2] and it seems that the plateau extends for the other type of
 335 soils.



336

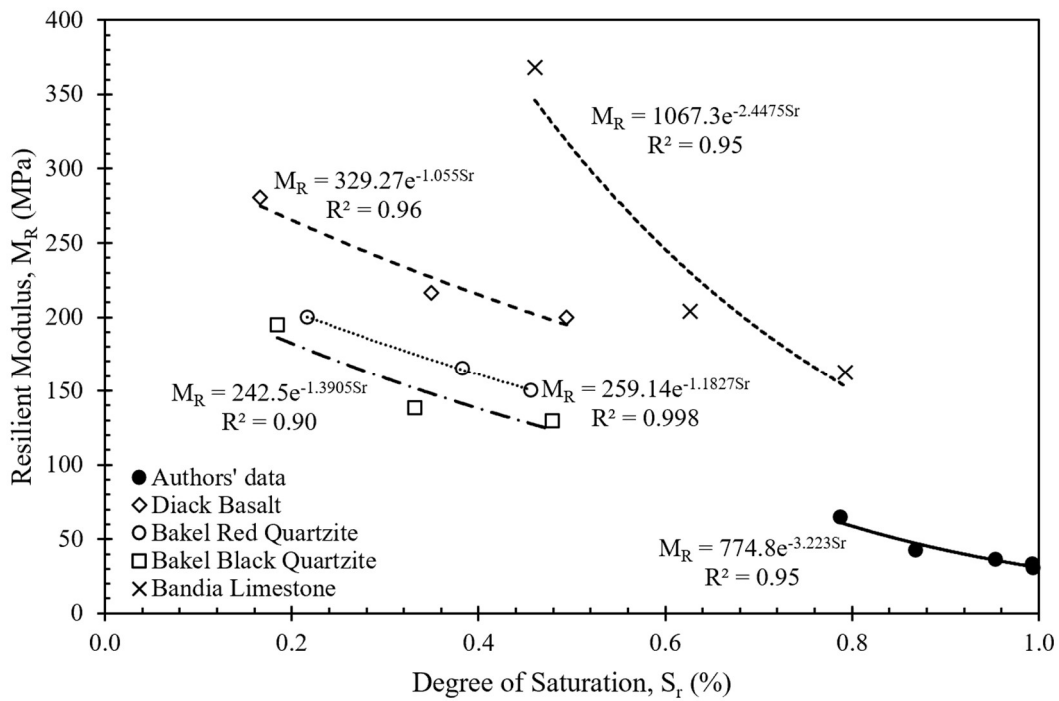
337 **Fig. 9.** Resilient modulus as a function of degree of saturation and matric suction on a
 338 semi-logarithmic scale.

339



340

(a)



341

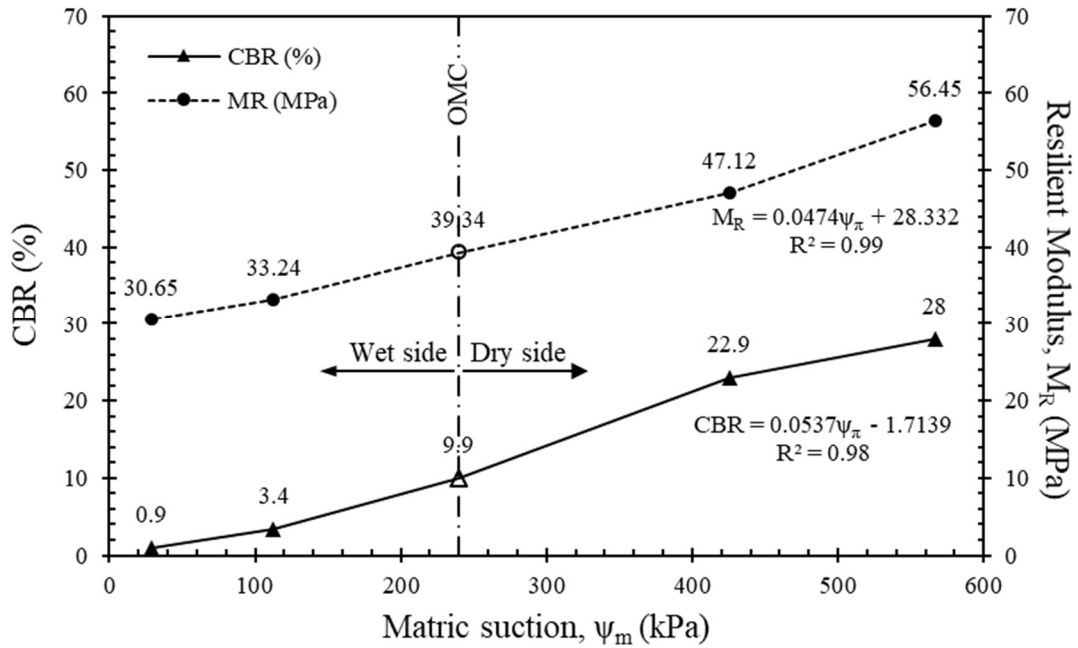
(b)

342 **Fig. 10.** Resilient modulus as a function of (a) matric suction and (b) degree of
 343 saturation.

344

345 **Resilient Modulus and CBR Relationships**

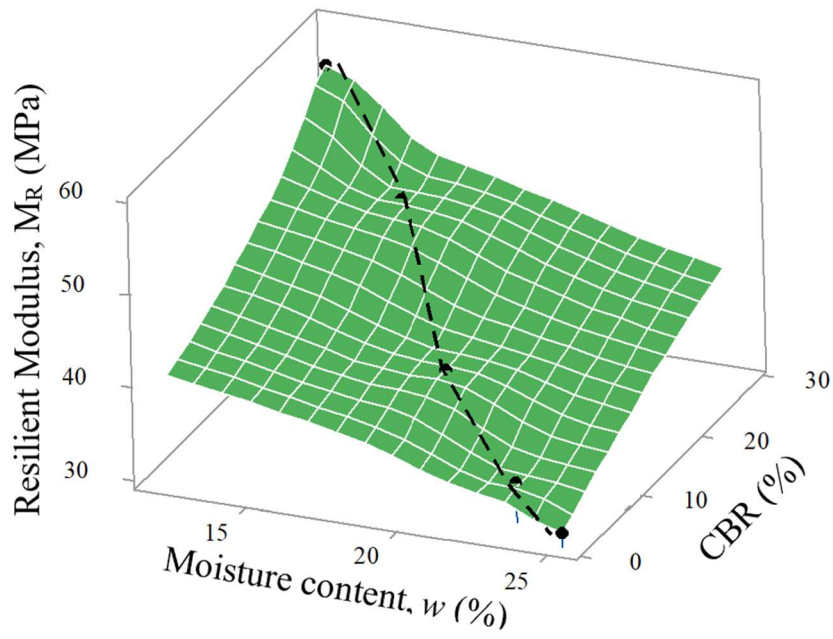
346 The evolution of the CBR and resilient modulus values based on matric suction
347 was drawn as presented in Fig. 11. Linear regression was observed for both CBR and
348 M_R against matric suction. At the wetter region prior to compacted at OMC, CBR and
349 MR values were increasing gradually at 30.65% and 33.24%, respectively. However,
350 when the soil was compacted at water content dryer than OMC, the CBR and MR value
351 increase tremendously to 28 % and 56.45 MPa, respectively. This seems that the
352 change in both M_R and CBR values are more sensitive toward the dry side. Thus, it is
353 interesting to note that the increment percentage for both CBR and M_R values are
354 almost similar at the wetter and dryer region of matric suction. Both CBR and M_R
355 values are expected to increase linearly beyond the compacted matric suction of 566.6
356 kPa. This finding is comparable to [6] for compacted kaolin. A one to one relationship
357 was also observed from this figure, with the reduction of M_R and CBR values across
358 the plane, it seems there is a consistent reduction in both parameters when it move to
359 the wet side. If the soil is compacted at the slightly dry side of the compacted range lie
360 within the 98% of maximum dry unit weight, the small change in the moisture content
361 (~3.5%) have substantial change in the results of M_R .
362



363
 364 **Fig. 11.** Evolution of the CBR and M_R values based on matric suction at five different
 365 moisture contents.
 366

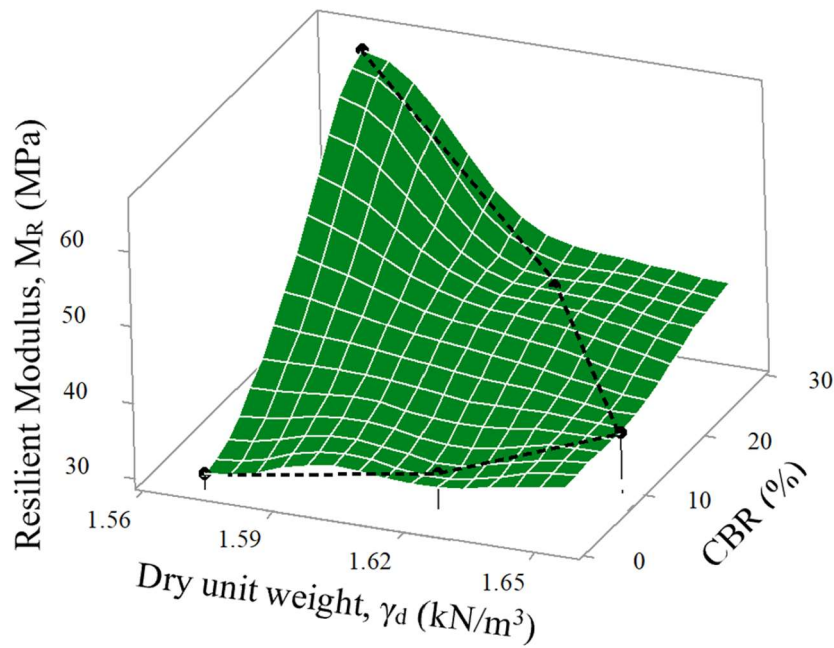
367 The discussion from the above findings can further established through multilinear
 368 regression model. The relationship of moisture content, dry unit weight, CBR and M_R
 369 was plotted in 3D surface plot shown in Fig. 12 (a) and (b). To explore the potential
 370 relationship between these three variables, the 3D surface plot was interpolated using
 371 MINITAB 17 statistical software. Minitab 17 surface plots response (z) values at the
 372 x-y intersections of an evenly-spaced mesh. If the x- and y-values are evenly spaced,
 373 Minitab 17 plots the z-values at the x-y intersections. If the x- and y-values are not
 374 evenly spaced, Minitab interpolates (estimates) the z-values at the intersections of a
 375 regular 15 by 15 mesh with the same x- and y-ranges as the data. In the case of this
 376 study, the three variables are not evenly space, therefore Minitab 17 interpolates the
 377 data using Distance method instead of Akima's polynomial method. Distance method
 378 works well in for this analysis as it estimate z within the range of the dataset for x and
 379 y. Whereas Akima's polonomial method does not give desired effect for this analysis
 380 as it uses a fifth-order polynomial which can only estimate z-values at x-y positions

381 beyond the available dataset that are too large or small. M_R is the response values
382 represented by z-axis whereas CBR and moisture content were plotted on the x- and y-
383 scales, respectively as the predictor factors. Fig. 12 (a) shows a rising ridge surface of
384 CBR and moisture content which have substantial effect on the resilient modulus. It
385 can also be observed that when either factors (CBR or moisture content) were
386 increasing at the same time leads to an increase in M_R . This phenomenon does not
387 occur in the case for dry unit weight. Both M_R and CBR values decreased moderately
388 to 39.34 MPa and 9.9 %, respectively for soil compacted at wet side of OMC,
389 regardless of the dry unit weight imparted. Fig. 12 (b) shows the 3D surface plot for
390 three different variables (M_R , γ_d and CBR) where resilient modulus and CBR values
391 are not entirely influenced by dry unit weight. As can be seen from this figure,
392 specimen prepared at the same dry unit weight was observed to have very significant
393 different in the resilient modulus and CBR values. In spite of compacted at the similar
394 dry unit weight over a wide range of moisture content, the strength and potentially its
395 stiffness of the compacted soil can behave very differently.
396



(a)

397



(b)

398

399 **Fig. 12.** Surface plot of three variations on: (a) Resilient modulus, moisture content
 400 and CBR; (b) Resilient modulus, dry unit weight and CBR.

401

402 These 3D surface plots are useful for establishing the regression model for M_R
 403 value. The nonlinear multiple regression model established for M_R as a function of

404 CBR and w $\{M_R = f(\text{CBR}, w)\}$ as shown in Eq. (7) is having coefficient of
405 determination of 0.99.

$$406 \quad M_R = 75.1 + 0.063 \text{ CBR} - 1.81w \quad (7)$$

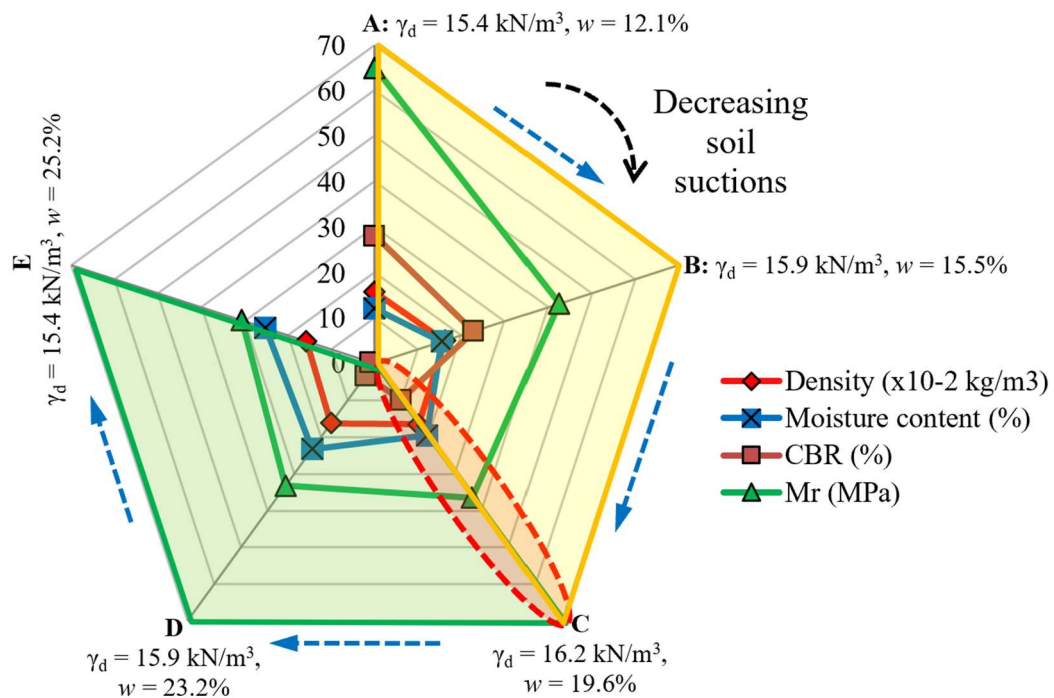
407 Where w and CBR value are presented in percentage.

408 Conversely, the nonlinear regression analysis of the three parameters for $M_R = f(\text{CBR},$
409 $\gamma_d)$ yields the following equation $\{vide \text{ Eq. (8)}\}$ with a high coefficient of determination
410 of 0.97, which is above 0.7 indicating relatively good fit according to Lim (2015).

$$411 \quad M_R = 52.4 + 0.864 \text{ CBR} - 1.41 \gamma_d \quad (8)$$

412 These factors are further summarized graphically in the polar chart shown in [Fig.](#)
413 [13](#). The five axes represent five different type of soil specimen prepared at different
414 moisture content and dry unit weight and tested with CBR and M_R with lowest value
415 moving towards the graph's centre and highest value appear towards the periphery. It
416 can be seen that with the decrease in soil matric suction, both CBR and M_R value tend
417 to move further away from the periphery indicating a decrease in the value. The red
418 circle with dashed line presenting the soil parameter compacted at optimum moisture
419 content and maximum dry density, whereas the yellow cluster indicate the drying side
420 and green cluster indicate the wetter side.

421



422

423 **Fig. 13.** Polar chart. The five axes represent five types of specimens prepared at
 424 different moisture content and dry density and tested with CBR and M_R with lowest
 425 value moving towards the graph's centre and highest value appear towards the
 426 periphery.

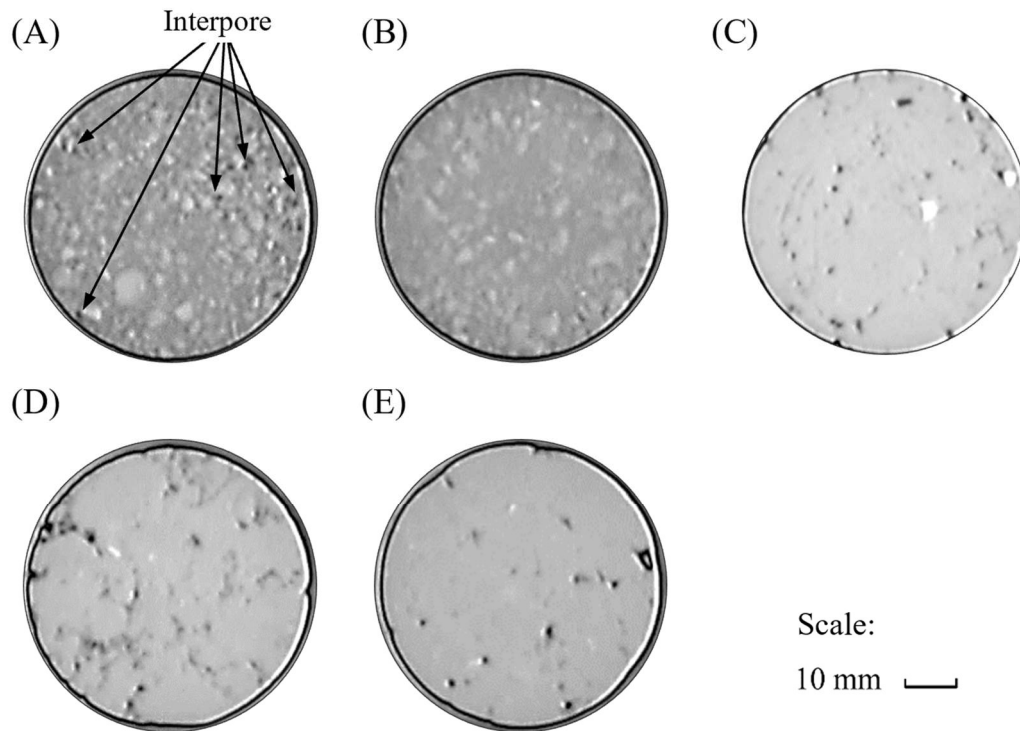
427

428 Soil Macrostructure

429 The CT-scanning has been carried out in this study to examine the macrostructural
 430 changes of soil compacted at different moisture content and dry unit weight. The CT-
 431 scanning was performed on the soil surface on both side of the sample. The structural
 432 changes observed in the compacted soils were evaluated in terms of macroporosity
 433 (inter-aggregate pores), by examining the differences in the greyscale of the images.
 434 Varying grayscale values represent sediment, water and void space. Presented herein,
 435 denser materials are represented as lighter grayscale values with the voids showing the
 436 darkest. For instance, white and grey areas correspond to sand particles and
 437 aggregations, respectively. Whereas dark areas correspond to air-filled and water-filled

438 pores. Similar technique was adopted by [35]. As illustrated in Fig. 14, specimen (A)
439 compacted at 12.1% of water content shows distinct aggregations (grey areas) with
440 large interpores (a mixed of water- and air-filled areas). While as the water content
441 increases to 15.5% for specimen (B), aggregations were observed with less air-filled
442 areas. There is an improved orientation of particles and a corresponding reduction in
443 size of voids as water content increase from specimen (A) to (B) as shown in the CT-
444 scan images. As the soil compacted to its OMC, water replaces the pores and this
445 further leads to a flocculation of the soil particles as shown in (C). This phenomenon
446 is observed to be in agreement with the findings hypothesized by Ajdari et al. (2013)[7]
447 and Lim et al. (2021)[42] . With higher bearing capacity and stiffness values observed
448 at the dryer site where compacted soils were observed to be flocculated
449 (compressibility reduces) through quantitative analysis, this phenomenon thus further
450 justify and in congruent with the findings reported in Lim et al. (2021)[36].

451 When the soil is compacted at wet side of optimal, as illustrated in (D) and (E),
452 these compacted soils have the opposite characteristics of the soil compacted at dry
453 side of the optimum water content. Soil compacted at water content higher than the
454 optimum water content results in a relatively weak matrix soil structure. At this point,
455 the aggregations fused slightly to form a more “matrix-dominated” macrostructure
456 during compaction. This gives a significant reduction in CBR and resilient modulus
457 values. These compacted soils exhibit a soil structure dominated by large amount of
458 macropores (i.e. the whiter areas). As soil compacted to a higher water content of 0.252
459 as shown in CT-scanned image (E), the micropores are observed to have moderately
460 lost to nearly absent. The studying of specimen prepared beyond the optimum moisture
461 content reveals a decrease in the number of connected voids filled with air,
462 consequently, matric are developed as a result.



464

465 **Fig. 14.** CT-scan images of compacted specimens at different moisture content: (a) w
 466 = 12.1%, (b) w = 15.5%, (c) w = 19.6%, (d) w = 23.2%, (e) w = 25.2%, representing
 467 five distinct of regions of aggregation.

468

469 Regardless of the effect of compaction, increasing soil moisture increased
 470 interpore volume [37]. When soils were compacted at the wet side of OMC, with the
 471 increased in moisture content, the aggregations become deformable and gradually tend
 472 to be more matrix-dominated macrostructure during compaction [34]. When the soils
 473 are compacted at dry side of OMC, distinct aggregations were observed, typically
 474 results in a flocculated and aggregated soil structure having random particle
 475 orientations, this mirrors the observations in considerable higher matric suction and
 476 higher CBR as well as resilient modulus values discussed above. It is thus worth noting
 477 that macrostructure changes associated with the increase in moisture content under
 478 different dry densities are possibly the reasons for the increase in the soil suction, M_R

479 and CBR values. This indicates that M_R and CBR exhibits a strong dependency on the
480 soil structure, as outlined in studies on compacted soil by Heitor et al. (2013[34]).
481 Nonetheless, it is recommended that the physical characterisation of compacted soil
482 using CT scan should be quantitatively analysed in terms of its saturated hydraulic
483 conductivity (K-Sat, cm h^{-1}), air permeability (K-Air, cm^2) and relative diffusivity for
484 He [38], among others for further research study.

485

486 **Conclusions**

487 Under unsaturated conditions, the effect of matric suction on the behaviour of soil
488 resilient modulus and CBR are of key importance. The results of a laboratory testing
489 programme allowed to examine the hysteretic behaviour of the soil suction on resilient
490 modulus and CBR of compacted Ballina clay along dryer and wetter region across a
491 compaction energy. The study also reiterates a common assumption in practice that
492 there is intimate relationship between the compaction characteristics (i.e. moisture
493 content and dry unit weight), soil suction and resilient modulus as well as CBR. It was
494 also noted that the stiffness of the compacted soil was significantly affected by the
495 water content. There is a one-to-one relationship observed with the reduction of M_R
496 and CBR across the evolution plane based on matric suction. This seems there is a
497 consistent reduction in both parameters when it moves to the wet side ($w > 19.6\%$). Both
498 M_R and CBR are relatively insensitive at the wet side. If small water content is change
499 in the field, it is expected not likely to affect strongly on the value of M_R and CBR (9
500 MPa and 8%, respectively). However, if small change ($\sim 3.5\%$) in the water content in
501 the dry side, a dramatic change will be expected for both M_R and CBR values (18 MPa
502 and 18 CBR, respectively). This also reveals that matric suction in soil contribute
503 significantly to the stiffness and strength of the soil. However, suction is lost when soil

504 absorbs water. This occurs in the field through water infiltration during rainfall. CT
505 scan results reveals that increasing soil moisture increased the interpores volume. Soils
506 compacted at the wet side of OMC impart that the aggregations became more
507 compressible and present probable matrix-dominated macrostructure during
508 compaction. While soils compacted at dry side of OMC yield distinct aggregations
509 owing to the flocculated and aggregated soil structure with random particle orientations
510 which mirror the observations in considerable higher matric suction and higher CBR
511 as well as resilient modulus values. Generally, notable correspondence can be found
512 between the soil suction, the water content, resilient modulus and CBR of compacted
513 Ballina clay. This study is limited to evaluating the variation of CBR and resilient
514 modulus of compacted Ballina clay as a function of total suction and matric suction in
515 the laboratory. Further investigation is required to study the influence of soil suction
516 on CBR and resilient modulus on soil compacted at different energy level.

517

518 **Acknowledgment**

519 This study has been conducted under the auspices of a funded Australian Research
520 council project. Authors gratefully acknowledge financial assistance. This study was
521 conducted while the first author was at the University of Wollongong, the use of the
522 facilities of the Centre for Geomechanics and Railway Engineering are
523 gratefully acknowledged. The first author would also like to thank Probase
524 Manufacturing Sdn. Bhd. for the main financial support for her study carried out in
525 Australia. This work was also supported by Shandong Excellent Young Scientists
526 Fund Program (Overseas) (2022HWYQ-016) and Shandong Provincial Natural
527 Science Foundation (ZR2021QE254).

528 **References**

- 529 [1] Wan, A. W. L., Gray, M. N., and Graham, J. 1995. On the relation of suction,
530 moisture content, and soil structure in compacted clays, *in proceeding of the First*
531 *International Conference on Unsaturated Soils*, UNSAT-95, Paris, pp. 215–222
- 532 [2] Ba, M., Nokkaew, K., Fall, M., & Tinjum, J. M. (2013). Effect of matric suction
533 on resilient modulus of compacted aggregate base courses. *Geotechnical and*
534 *Geological Engineering*, 31(5), 1497-1510.
- 535 [3] Vanapalli, S. K., & Han, Z. (2014). Application of the unsaturated soil mechanics
536 in the design of pavements. In *Proceedings of the 6th International Conference on*
537 *Unsaturated Soils, Sydney, Australia* (pp. 1799-1805).
- 538 [4] Kim, H., Ganju, E., Tang, D., Prezzi, M., & Salgado, R. (2015). Matric suction
539 measurements of compacted subgrade soils. *Road Materials and Pavement*
540 *Design*, 16(2), 358-378.
- 541 [5] Transportation Officials. (1993). *AASHTO Guide for Design of Pavement*
542 *Structures, 1993* (Vol. 1).
- 543 [6] Mirzaii, A., & Negahban, M. (2016). California bearing ratio of an unsaturated
544 deformable pavement material along drying and wetting paths. *Road Materials*
545 *and Pavement Design*, 17(1), 261-269.
- 546 [7] Ajdari, M., Habibagahi, G., & Masrouri, F. (2013). The role of suction and degree
547 of saturation on the hydro-mechanical response of a dual porosity silt–bentonite
548 mixture. *Applied Clay Science*, 83, 83-90.
- 549 [8] Dong, X. X., Chen, Y. G., Ye, W. M., & Cui, Y. J. (2020). Effect of initial suction
550 on the stiffness and strength of densely compacted Gaomiaozhi bentonite. *Applied*
551 *Clay Science*, 194, 105696.

- 552 [9] Kim, D., & Kim, J. R. (2007). Resilient behavior of compacted subgrade soils
553 under the repeated triaxial test. *Construction and Building Materials*, 21(7), 1470-
554 1479.
- 555
- 556 [10] Nowamooz, H., Chazallon, C., Arsenie, M. I., Hornyh, P., & Masrouri, F. (2011).
557 Unsaturated resilient behavior of a natural compacted sand. *Computers and*
558 *Geotechnics*, 38(4), 491-503.
- 559 [11] Sawangsuriya, A., Edil, T. B., & Bosscher, P. J. (2008). Modulus-suction-
560 moisture relationship for compacted soils. *Canadian Geotechnical Journal*, 45(7), 973-
561 983.
- 562 [12] Sukumaran, B., Kyatham, V., Shah, A., & Sheth, D. (2002, May). Suitability
563 of using california bearing ratio test to predict resilient modulus. In *Proceedings:*
564 *Federal aviation administration airport technology transfer conference* (p. 9).
- 565 [13] Mendoza, C., & Caicedo, B. (2018). Elastoplastic framework of relationships
566 between CBR and Young's modulus for granular material. *Road Materials and*
567 *Pavement Design*, 19(8), 1796-1815.
- 568 [14] Garg, N., Larkin, A., & Brar, H. (2009). A comparative subgrade evaluation using
569 CBR, vane shear, light weight deflectometer, and resilient modulus tests.
570 In *Proceedings of the 8th International Conference on the Bearing Capacity of*
571 *Roads, Railways and Airfields* (Vol. 5, pp. 57-64).
- 572 [15] Leung, G. L. M., Wong, A. W. G., & Wang, Y. H. (2013). Prediction of resilient
573 modulus of compacted saprolitic soils by CBR approach for road pavement
574 subgrade: a re-examination. *International Journal of Pavement*
575 *Engineering*, 14(4), 403-417.

- 576 [16] Howard, A. K. (1984). The revised ASTM standard on the unified classification
577 system. *Geotechnical Testing Journal*, 7(4), 216-222.
- 578 [17] Indraratna, B., Perera, D. and Rujikiatkamjorn, C. & Kelly, R. (2014). Soil
579 disturbance analysis due to vertical drain installation. *Proceedings of the*
580 *Institution of the Institution of Civil Engineers – Geotechnical Engineering*,
- 581 [18] Pineda, J. A., Suwal, L. P., Kelly, R. B., Bates, L., & Sloan, S. W. (2016).
582 Characterisation of Ballina clay. *Géotechnique*, 66(7), 556-577.
- 583 [19] Google Maps, 2017. *Anglia Ruskin University: Chelmsford Campus*, 1:1.500.
584 Google Maps [online] Available through: ARU Library <<http://library.aru.ac.uk>>
585 [Accessed 6 August 2022].
- 586 [20] AS 1289.5.1.1:2003, Methods of Testing Soils for Engineering Purposes –
587 Determination of the Dry Density/Moisture Content Relation of a Soil Using
588 Standard Compactive Effort, Standards Australia.
- 589 [21] Chen, Q., & Indraratna, B. (2015). Deformation behavior of lignosulfonate-treated
590 sandy silt under cyclic loading. *Journal of Geotechnical and Geoenvironmental*
591 *Engineering*, 141(1), 06014015.
- 592 [22] Su, Y., Cui, Y. J., Dupla, J. C., & Canou, J. (2022). Soil-water retention behaviour
593 of fine/coarse soil mixture with varying coarse grain contents and fine soil dry
594 densities. *Canadian Geotechnical Journal*, 59(2), 291-299.
- 595 [23] Davish P., Labuz J.F., Guzina B., Drescher A. Small strain and resilient modulus
596 testing of granular soils (Final Report). Minesota Departmet of transportation
597 research services section, 2004.
- 598 [24] ASTM (2013). Standard test method for load controlled cyclic triaxial strength of
599 soil. ASTM D 5311/D5311-M-13, American Society of Testing materials. West
600 Conshohoken, PA.

- 601 [25] ASTM (2005). Standard test method for California bearing ratio of laboratory-
602 compacted soils. ASTM D1883-05. American Society of Testing materials. West
603 Conshohoken, PA.
- 604 [26] ASTM (2003). Standard test method for measurement of soil potential (suction)
605 using filter paper method. ASTM standard D 5298 Annual Book of Standards.
606 American Society of Testing Materials. West Conshohoken, PA.
- 607 [27] Fredlund, D. G. and Rahardjo, H. (1993). Soil mechanics for unsaturated soils.
608 *New York: John Wiley & Sons, Inc.*
- 609 [28] Leong, E. C., He, L., & Rahardjo, H. (2002). Factors affecting the filter paper
610 method for total and matric suction measurements. *Geotechnical Testing*
611 *Journal*, 25(3), 322-333.
- 612 [29] Alshibli, K. A., Alramahi, B. A., & Attia, A. M. (2006). Assessment of spatial
613 distribution of porosity in synthetic quartz cores using microfocus computed
614 tomography (μ CT). *Particulate science and technology*, 24(4), 369-380.
- 615 [30] Vulliet, L., Schrefler, B., & Laloui, L. (2002). *Environmental Geomechanics*.
616 EPFL Press.
- 617 [31] Delage, P., & Graham, J. (1996). Mechanical behaviour of unsaturated soils:
618 understanding the behaviour of unsaturated soils requires reliable conceptual
619 models. In *PROCEEDINGS OF THE FIRST INTERNATIONAL CONFERENCE*
620 *ON UNSATURATED SOILS/UNSAT'95/PARIS/FRANCE/6-8 SEPTEMBER 1995*.
621 *VOLUME 3*.
- 622 [32] Cabalar, A. F., & Mustafa, W. S. (2017). Behaviour of sand–clay mixtures for road
623 pavement subgrade. *International Journal of Pavement Engineering*, 18(8), 714-
624 726.

- 625 [33] Liang, W. Y., Yan, R. T., Xu, Y. F., Zhang, Q., Tian, H. H., & Wei, C. F. (2021).
626 Swelling pressure of compacted expansive soil over a wide suction range. *Applied*
627 *Clay Science*, 203, 106018.
- 628 [34] Heitor, A., Indraratna, B., & Rujikiatkamjorn, C. (2013). Laboratory study of
629 small-strain behavior of a compacted silty sand. *Canadian Geotechnical*
630 *Journal*, 50(2), 179-188.
- 631 [35] Rees, E. V., Priest, J. A., & Clayton, C. R. (2011). The structure of methane gas
632 hydrate bearing sediments from the Krishna–Godavari Basin as seen from Micro-
633 CT scanning. *Marine and Petroleum Geology*, 28(7), 1283-1293.
- 634 [362] Lim, S. M., Yao, K., Jiang, Y., Lim, Z. C., & Bakar, I. H. (2021). Geotechnical
635 characteristics of lateritic clay admixed with biomass silica stabiliser. *Journal of*
636 *Cleaner Production*, 321, 129008.
- 637 [37] Menon, M., Jia, X., Lair, G. J., Faraj, P. H., & Bland, A. (2015). Analysing the
638 impact of compaction of soil aggregates using X-ray microtomography and water
639 flow simulations. *Soil and Tillage Research*, 150, 147-157.
- 640 [38] Grevers, M. C. J., JONG, E. D., & St. Arnaud, R. J. (1989). The characterization
641 of soil macroporosity with CT scanning. *Canadian Journal of Soil Science*, 69(3),
642 629-637.